

PAPER • OPEN ACCESS


Efficient quantum state tracking in noisy environments

To cite this article: Markus Rambach *et al* 2023 *Quantum Sci. Technol.* **8** 015010

View the [article online](#) for updates and enhancements.

You may also like

- [Cooperative emission spectra as an efficient key probe of qubits pair entanglement along with field state tomography: an effective response to nonlinearity and classical drive power](#)
M S Ateto
- [A single-atom quantum memory in silicon](#)
Solomon Freer, Stephanie Simmons, Arne Laucht *et al.*
- [Comparison of confidence regions for quantum state tomography](#)
Jessica O de Almeida, Matthias Kleinmann and Gael Sentis

 **kiutra**

Easy-to-use and Helium-3 free
cryogenics solutions

LEARN MORE

Quantum Science and Technology



PAPER

Efficient quantum state tracking in noisy environments

OPEN ACCESS

RECEIVED
31 July 2022

REVISED
14 October 2022

ACCEPTED FOR PUBLICATION
4 November 2022

PUBLISHED
16 November 2022

Original Content from
this work may be used
under the terms of the
[Creative Commons
Attribution 4.0 licence](#).

Any further distribution
of this work must
maintain attribution to
the author(s) and the title
of the work, journal
citation and DOI.



Markus Rambach^{1,*} , Akram Youssry^{2,3} , Marco Tomamichel⁴ and Jacqueline Romero¹

¹ Australian Research Council Centre of Excellence for Engineered Quantum Systems & School of Mathematics and Physics, Brisbane, QLD 4072, Australia

² University of Technology Sydney, Centre for Quantum Software and Information, Ultimo, NSW 2007, Australia

³ Quantum Photonics Laboratory and Centre for Quantum Computation and Communication Technology, RMIT University, Melbourne, VIC 3000, Australia

⁴ Department of Electrical and Computer Engineering & Centre for Quantum Technologies, National University of Singapore, Singapore 119077, Singapore

* Author to whom any correspondence should be addressed.

E-mail: m.rambach@uq.edu.au

Keywords: quantum control, AI, machine learning, quantum tomography, qudit

Abstract

Quantum state tomography, which aims to find the best description of a quantum state—the density matrix, is an essential building block in quantum computation and communication. Standard techniques for state tomography are incapable of tracking changing states and often perform poorly in the presence of environmental noise. Although there are different approaches to solve these problems theoretically, experimental demonstrations have so far been sparse. Our approach, matrix-exponentiated gradient (MEG) tomography, is an online tomography method that allows for state tracking, updates the estimated density matrix dynamically from the very first measurements, is computationally efficient, and converges to a good estimate quickly even with very noisy data. The algorithm is controlled via a single parameter, its learning rate, which determines the performance and can be tailored in simulations to the individual experiment. We present an experimental implementation of MEG tomography on a qutrit system encoded in the transverse spatial mode of photons. We investigate the performance of our method on stationary and evolving states, as well as significant environmental noise, and find fidelities of around 95% in all cases.

1. Introduction

Characterising quantum systems becomes increasingly important as quantum technologies begin to scale up. Experiments often require verification of the prepared quantum state and detection of errors as the state evolves, e.g. through deliberate evolution or environmental perturbations. Thus, quantum state tomography (QST)—finding the density matrix that best describes a quantum system—is a task central to quantum information processing. However, QST is notoriously resource-intensive [1]. Reconstructing the d -by- d density matrix of a d -dimensional quantum system up to a fixed precision requires $O(d^2)$ parameters that can only be obtained after measuring at least $O(d^3)$ copies of the quantum state [2]. Most common algorithms for QST (e.g. maximum likelihood estimation [3] and least squares regression [4]) require a tomographically complete set of measurements and are done in post-processing, thus precluding real-time control of experiments based on the QST results.

Current experimental realisations of quantum devices often suffer from perturbations that change over time which might happen faster than a complete set of measurements can be performed. It might also be of interest to the experimentalist to observe the evolution of states in an experiment. Both these scenarios require online QST—learning algorithms that continuously update the estimate of the state description [5], and thus enable real-time control and diagnosis of errors. Recent proposals for this include Bayesian approaches [6, 7], adaptive measurements [8–11], and machine learning techniques [11–15]. All these techniques are also related to continuous learning [16, 17]—weak measurements over time to characterise a systems evolution, motivated by feedback control to correct errors—and Hamiltonian

identification/learning [18, 19]—algorithms to determine Hamiltonian parameters governing the dynamics or unknown structures in the system, motivated by distinguishing and quantification of errors.

Moreover, arbitrary noise from the environment or from imperfect measurements can easily surpass the signal strength in experiments. This degrades our ability to accurately estimate the quantum state, hence the robustness of techniques is crucial. Usual efforts to circumvent this issue experimentally try to improve the signal-to-noise ratio (SNR), which is not always feasible or indeed possible. Some theoretical work exist, e.g. [20, 21] where the noise is formalised into the measurement, or [22] where an algorithm robust to noisy data is designed. However, none of these consider dynamical states and we are not aware of any experimental demonstrations.

Here, we focus on QST using the matrix-exponentiated gradient (MEG) method [13, 14]. The reduced computational complexity per iteration of MEG, $O(d^3)$ in contrast to maximum likelihood and least squares regression which are both $O(d^4)$, makes it a good candidate for online QST. The MEG algorithm is also efficient—it does not require a full set of measurements for each state estimate—and robust—simulations show convergence even with very noisy measurements. Additionally, the MEG update rule ensures that the estimated state is physical (i.e. a positive-semi definite density matrix), which is generally not guaranteed in most tomography methods unless the estimate is projected back into the physical space, causing a bias towards low-rank states in the estimator [23].

In this work, we experimentally demonstrate real-time, online QST based on MEG using a high-dimensional ($d > 2$) quantum system encoded in the transverse spatial mode of single photons. We achieve fidelities of up to 95% even in the presence of significant noise due to statistical fluctuations (e.g. very low count rates) and environmental effects (e.g. an ambient light source). To our knowledge, this is the first experimental $O(d^3)$ online tomography implementation to date. A similar $O(d^3)$ online algorithm has been proposed recently [15], however, an experiment is still lacking.

2. Methods

2.1. Experimental setup and measurement

The quantum states are encoded in the transverse spatial mode—the shape—of single photons. We describe these modes in the Laguerre–Gaussian basis $\{|l_i, p_i\rangle\}$ [24], where each randomly chosen state is given by the superposition $|\psi\rangle = \sum_i c_i |l_i, p_i\rangle$ (with $\sum_i |c_i|^2 = 1$). For the investigated qutrits in the experiment we use the three logical basis states $\{|0\rangle \equiv |-1, 0\rangle, |1\rangle \equiv |0, 2\rangle, |2\rangle \equiv |1, 0\rangle\}$, keeping the Gouy phase of the same order and therefore preventing the shape from rotating as the photons propagate [25]. The experiment is conducted with highly attenuated CW laser light (Thorlabs, mean photon number $|\alpha|^2 = 0.01$) together with two spatial light modulators (SLM, Meadowlark Optics) and a single photon detector (Perkin-Elmer, ~ 100 Hz dark count rate). The first SLM is used to prepare the *unknown* quantum state $|\psi_t\rangle$ via a hologram that changes phase and amplitude of the initial state $|l=0, p=0\rangle$ from the laser source. A second hologram displayed on the other SLM is then measuring the state $|\psi_m\rangle$ from one randomly chosen basis set (see section 2.3 for details). Finally, a single-mode fibre and the detector are acting as a local filter with the number of detected photons proportional to the overlap $|\langle \psi_m | \psi_t \rangle|^2$ between the prepared and measured mode. We note that, although all experiments were performed on a qutrit ($d=3$) as proof of principle, the setup is capable of preparing and measuring much higher dimensions as shown in previous work [26]. The schematic, details, and characterisation of this simple but effective prepare-and-measure experiment are described in [26].

2.2. Algorithm overview

MEG tomography [13, 14] is an online algorithm adapted from machine learning techniques that can estimate and track quantum states. The idea is to construct an iterative procedure, in which an estimate $\hat{\rho}_t$ of the (mixed or pure) quantum state at the iteration t is updated to a more accurate estimate $\hat{\rho}_{t+1}$, given a new measurement performed on the unknown quantum state. The MEG update rule [14] for the estimate $\hat{\rho}_{t+1}$ is given by:

$$\hat{\rho}_{t+1} = \frac{\exp(\log(\hat{\rho}_t) - \eta_t \nabla L_t)}{\text{tr} \exp(\log(\hat{\rho}_t) - \eta_t \nabla L_t)}, \quad (1)$$

where η_t is the learning rate, and L_t is the loss function,

$$L_t = (\text{tr}(\hat{\rho}_t X_t) - y_t)^2, \quad (2)$$

and its gradient is given by:

$$\nabla L_t = 2(\text{tr}(\hat{\rho}_t X_t) - y_t) X_t. \quad (3)$$

The pair (X_t, y_t) denotes the measurement record where X_t is the measurement operator and y_t is the experimentally obtained average value of measuring the state with operator X_t . The measurements have to be informationally complete as a requirement for performing any quantum tomography procedure. Therefore, at each iteration, a measurement operator X_t is chosen at random from a complete set of bases, and together with the measurement result y_t , the estimate of the state $\hat{\rho}_t$ is updated to $\hat{\rho}_{t+1}$. The learning rate η_t determines the weight given to the new obtained information at each iteration. For tomography on stationary states, η_t can be chosen to decrease continuously with the number of iterations while for online state tracking it needs to be constant or adaptive, depending on former measurement outcomes.

2.3. MEG estimation extensions

We generalised the originally proposed MEG in [14] to make it applicable to qudits ($d > 2$), and also introduced modifications to make the algorithm more suitable for our experiment.

2.3.1. Measurement schemes

We extended MEG to work with general higher-dimensional systems $d > 2$ and local Pauli measurements. We use two measurement schemes to perform our state estimation and online tracking. The first scheme is utilising Mutually Unbiased Bases (MUBs) [27], measurements that are optimal for extracting information [28]. For a d -dimensional quantum system, we have a maximum of $d + 1$ basis sets, each set consistent of d states. However, complete sets of MUBs are not known for every dimension and so it is important to also introduce a second scheme using generalised Pauli operators [29]. These operators are given by the set $\{u_{jk}, v_{jk}, w_l\}$:

$$u_{jk} = |j\rangle\langle k| + |k\rangle\langle j|, \quad 0 \leq j \leq k \leq d \quad (4a)$$

$$v_{jk} = -i|j\rangle\langle k| + i|k\rangle\langle j|, \quad 0 \leq j \leq k \leq d \quad (4b)$$

$$w_l = \sqrt{\frac{2}{l+1}} \left(-l|l\rangle\langle l| + \sum_{j=0}^l |j\rangle\langle j| \right) \quad 0 \leq l \leq d. \quad (4c)$$

The operators reduce to the Pauli and Gell-Mann matrices for $d = 2$ and $d = 3$, respectively. The total number of operators is $d^2 - 1$, and for each operator, there are d eigenstates that can be measured. The extension to generalised Pauli operators gives us eigenbases which are orthonormal and informationally complete, thus making the algorithm applicable to any dimension. Projective measurements of MUBs and eigenbases of Pauli operators are conveniently implemented in the experiment, thus making our setup ideal for testing the MEG algorithm.

2.3.2. Modified update rule

The learning rate is usually chosen to be adaptive to guarantee convergence in the case of noisy measurements as shown in [14]. However, upon exploring the effect of choosing different learning rates, we found that a constant learning rate is sufficient to obtain an estimate with the maximum possible accuracy obtainable given our experimental capabilities. Thus, we fix the learning rate to be $\eta_t = \eta = 5$.

The measurement schemes we use provide us with more information at each iteration. In the case of MUB measurements, we randomly select a basis at each iteration. In order to calculate the probabilities, we need to projectively measure all states of that basis for normalisation of the measurement counts. The same holds when we use generalised Pauli measurements, we still need to measure all the eigenstates of a given Pauli operator. Therefore, we modify the loss function to include multiple measurement results obtained at a given iteration as follows:

$$L_t = \sum_{i=1}^d \left(\text{tr}(\hat{\rho}_t X_t^{(i)}) - y_t^{(i)} \right)^2, \quad (5)$$

with gradient:

$$\nabla L_t = 2 \sum_{i=1}^d \left(\text{tr}(\hat{\rho}_t X_t^{(i)}) - y_t^{(i)} \right) X_t^{(i)}, \quad (6)$$

where $X_t^{(i)} = |\psi_i\rangle\langle\psi_i|$ is the projector of the i th state of the MUB (or eigenstate of the Pauli operator) basis that was randomly chosen at iteration t out of $d + 1$ (or $d^2 - 1$) possible bases, and $y_t^{(i)}$ is the measured

probability. Although this modification is motivated by how we perform our measurements, it is beneficial for many experimental platforms, where often several projective measurements are necessary to calculate probabilities.

Since we are restricting the experiments to pure states in our investigations—true for systems that have very high control over their preparation, we can increase the estimation accuracy using this prior information. The method we use is to project the state into the subspace of its largest eigenvalue, or equivalently, finding the pure state closest to our estimate in fidelity. We illustrate this method with an example: we can write the estimated density matrix $\hat{\rho}_t$ of a pure quantum state $|\phi_t\rangle$ in the form:

$$\hat{\rho}_t = \lambda |\phi_t\rangle\langle\phi_t| + (1 - \lambda) \hat{\rho}_{\text{noise}}, \quad (7)$$

where the parameter $\lambda \in [0, 1]$ indicates the noise strength, and $\hat{\rho}_{\text{noise}} = I_d/d$ is the completely mixed state representing the noise in the estimate, with I_d the d dimensional identity matrix. The special cases $\lambda = 0$ and $\lambda = 1$ correspond to the noiseless and completely noisy states respectively. Now, let $|\gamma_t\rangle$ be an eigenstate of $\hat{\rho}_t$ with eigenvalue γ_t , i.e. $\hat{\rho}_t |\gamma_t\rangle = \gamma_t |\gamma_t\rangle$. Then, we can write:

$$\gamma_t = \langle\gamma_t|\hat{\rho}_t|\gamma_t\rangle \quad (8a)$$

$$= \lambda \langle\gamma_t|\phi_t\rangle\langle\phi_t|\gamma_t\rangle + (1 - \lambda) \frac{\langle\gamma_t|I_d|\gamma_t\rangle}{d} \quad (8b)$$

$$= \lambda |\langle\gamma_t|\phi_t\rangle|^2 + \frac{1 - \lambda}{d}. \quad (8c)$$

From there, we can see that the maximum eigenvalue is:

$$\gamma_{t,\text{max}} = \lambda + \frac{1 - \lambda}{d}, \quad (9)$$

which is obtainable when there is maximum overlap between γ_t and ϕ_t , in the best case $|\langle\gamma_t|\phi_t\rangle|^2 = 1$, i.e. $|\gamma_t\rangle = |\phi_t\rangle$. This shows that the true pure state $|\phi_t\rangle$ is an eigenvector of the density matrix $\hat{\rho}_t$ corresponding to the maximum eigenvalue, in other words, closest to our estimator in fidelity. So, after each iteration we calculate the eigenvalues of the state estimate and select the corresponding eigenvector to be the estimate of the pure state $|\phi_t\rangle$ with density matrix $\hat{\rho}_\phi$. Finally, the infidelity

$1 - f(\hat{\rho}_\phi, \hat{\Omega}_\psi) = 1 - \left(\text{tr} \sqrt{\sqrt{\hat{\rho}_\phi} \hat{\Omega}_\psi \sqrt{\hat{\rho}_\phi}} \right)^2$ is used for benchmarking of the algorithm. Here, $f(\hat{\rho}_\phi, \hat{\Omega}_\psi)$ is

the fidelity and $\hat{\Omega}_\psi$ is the density matrix of the theoretical prepared state $|\psi_t\rangle$. Our results show convergence to the unknown state within experimental limitations, most prominently mode-dependent losses, in all investigated situations and even for excessive experimental noise. We note that MEG estimates a full density matrix and hence related parameters of interest (as sometimes used in other tomography schemes, e.g. shadow tomography [30, 31]) can be calculated with high accuracy.

3. Results

3.1. State estimation and online tracking

We investigated the qutrit ($d = 3$) state estimation and online tracking performance of MEG using mutually unbiased bases (MUBs) and generalised Pauli operator measurements, which makes the algorithm generic and applicable to higher dimensions. We also investigated the MEG performance in the presence of small and large statistical noise, and also environmental noise. In all cases we continuously evolve the prepared state in time following:

$$|\psi_t\rangle = \exp(-i\sigma\omega t)|\psi_0\rangle, \quad (10)$$

where σ is a Hermitian matrix and $\omega = \frac{1.3}{t_{\text{tot}}}$ the rate of change dependent on the total amount of iterations t_{tot} . The rate of change was chosen to allow the state to evolve to a minimum fidelity compared to the initial state and then back to its initial state. We studied three possible cases of σ : $0_{3,3}$ which is the 3-dimensional zero matrix, σ_z which is the generalised 3-dimensional Pauli Z matrix given by [29, 32]:

$$\sigma_z = \frac{1}{\sqrt{3}} \begin{pmatrix} 1 & 0 & 0 \\ 0 & 1 & 0 \\ 0 & 0 & -2 \end{pmatrix}, \quad (11)$$

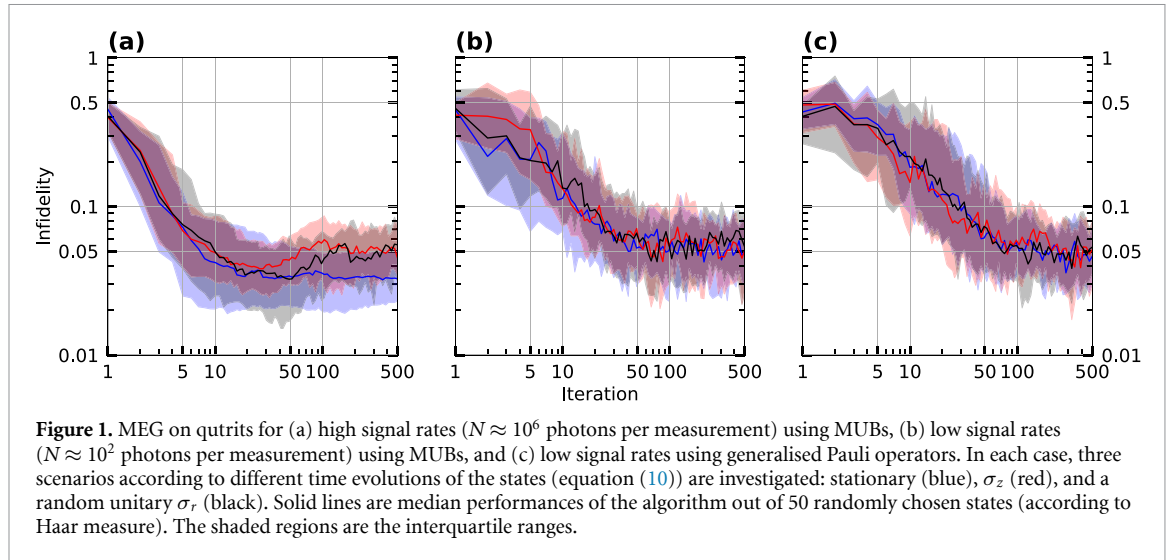


Table 1. MEG performance indicators. Top: iterations needed to reach 10% infidelity. Bottom: mean infidelity. All values achieved with a constant learning rate $\eta = 5$. Uncertainties are the boundaries of the interquartile ranges, i.e. a mean infidelity of $(5.3^{+3.2}_{-2.2})\%$ means that the middle 50%—between 25%–75%, sorted by their infidelity—of our investigated states showed infidelities between 3.1% and 8.5%.

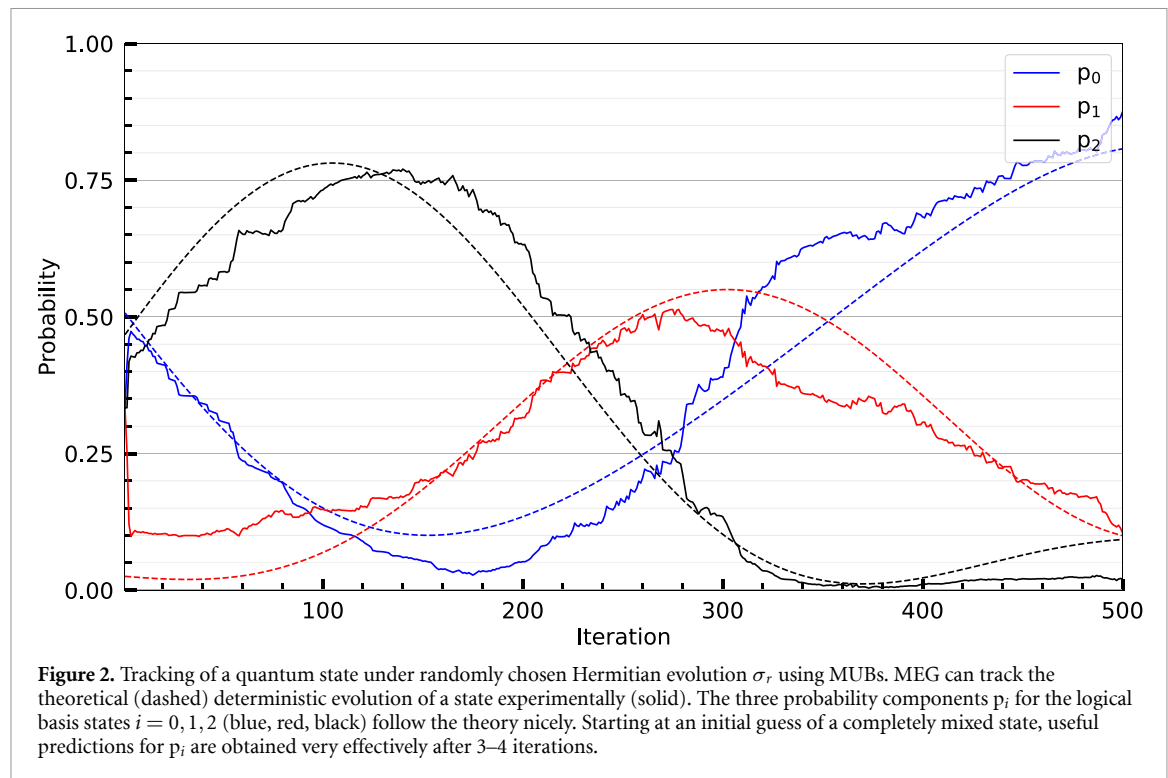
Signal rate (Hz)	MUB			Pauli operators		
	$\sigma = 0_{3,3}$	$\sigma = \sigma_z$	$\sigma = \sigma_r$	$\sigma = 0_{3,3}$	$\sigma = \sigma_z$	$\sigma = \sigma_r$
Iterations for infidelity < 10%						
10^2	14^{+17}_{-10}	13^{+26}_{-6}	16^{+26}_{-12}	30^{+32}_{-21}	23^{+68}_{-14}	24^{+38}_{-17}
10^6	4^{+2}_{-1}	4^{+3}_{-1}	4^{+4}_{-1}			
Mean infidelity (%)						
10^2	$5.3^{+3.2}_{-2.2}$	$5.4^{+3.4}_{-2.4}$	$5.6^{+3.4}_{-2.5}$	$4.9^{+2.8}_{-2.0}$	$5.4^{+3.5}_{-2.4}$	$5.0^{+3.3}_{-2.1}$
10^6	$3.4^{+1.8}_{-1.2}$	$5.1^{+2.2}_{-1.9}$	$4.7^{+2.3}_{-1.9}$			

and σ_r which is a general random Hermitian matrix. The zero matrix results in the identity evolution leaving the initial state stationary, while the other two matrices simulate a rotation in the Hilbert space of a qutrit. To ensure a fair comparison, the learning rate—a crucial parameter for performance and convergence of the algorithm—is kept constant at $\eta = 5$, which shows good performance in all cases albeit not optimal for $\sigma = 0_{3,3}$. The learning rate can be optimised individually, dependent on investigated scenario and physical system.

An initial baseline measurement using MUBs and high signal rates ($N \approx 10^6$ photons per measurement) is shown in figure 1(a). The high count rate ensures that statistical Poissonian distributed counting noise ($\Delta N = \sqrt{N} \approx 10^3$), background ($N_{\text{back}} \approx 50$) and dark counts ($N_{\text{dark}} \approx 100$), are negligible and do not deteriorate the performance. For this case, the algorithm finds density matrices with a median purity above 99.6% in all investigated scenarios, as to be expected for our system where we have a high degree of control over the state preparation. Since the fidelities in the experiments are very high, we plot the infidelity, $1 - f(\hat{\rho}_\phi, \hat{\Omega}_\psi)$, for clarity. The solid lines in figure 1(a) are the median infidelities of 50 randomly chosen states of qutrits (according to Haar measure), with the shaded regions bounded by the upper and lower quartile (50 ± 25)%.

In theory, MEG can estimate any quantum state with arbitrary precision and accuracy given an infinite amount of iterations. However, experimental imperfections such as misalignment and mode-dependent loss significantly limit the minimum infidelities achievable by QST algorithms (not just MEG). The infidelities for MEG listed in table 1 are similar to those obtained using other QST algorithms applied to our system, e.g. root-approach and maximum-likelihood estimators [33] where we set the rank to 1.

We next show the robustness of MEG to noise using MUBs, reducing the count rate per iteration to $N \approx 10^2$. This means that the values for Poissonian, dark, and background noise become comparable and play a significant role in state estimation and tracking. Robustness to statistical noise in the limit of a small number of repeated preparations of the unknown state—here the number of photons—is especially interesting for systems like ions and superconducting qubits, as the preparation is considerably more time



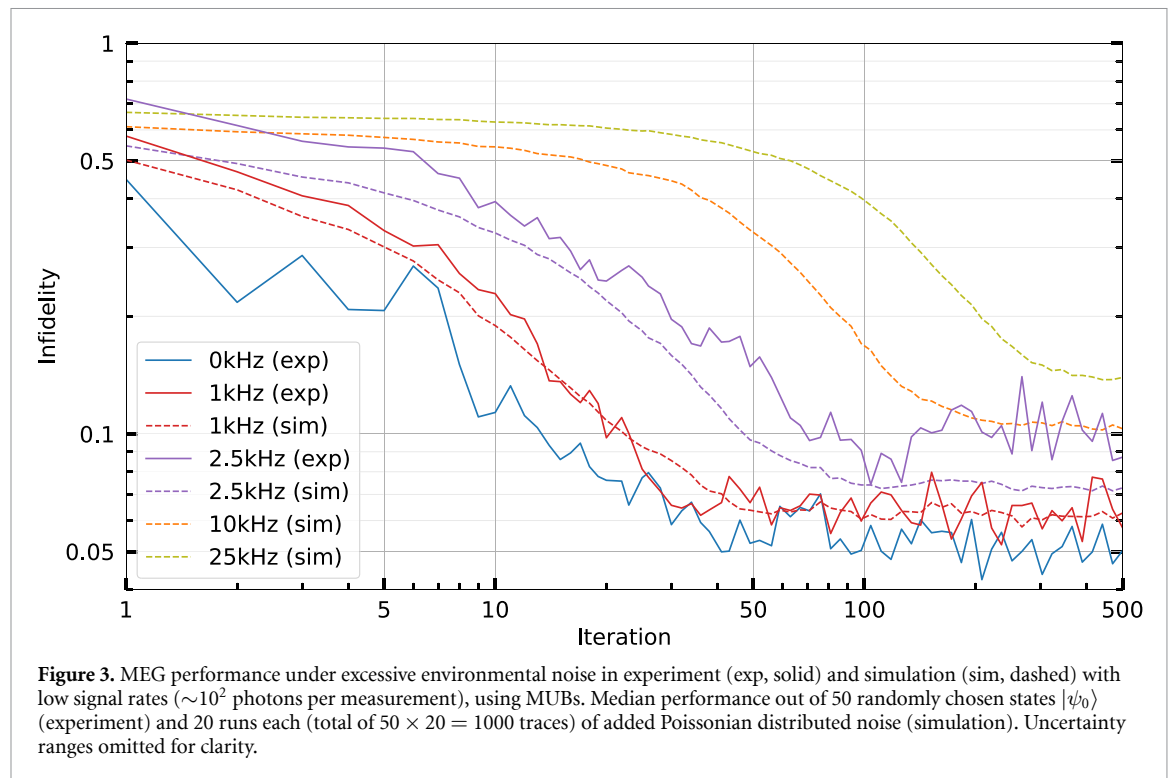
consuming compared to our system. Again, we benchmark the performance of MEG by calculating the infidelity in each iteration, see figure 1(b). State estimation and online tracking are in excellent agreement with an overall mean infidelity $\sim 5.5\%$, slightly higher than in the high count rate case, but well within the uncertainty bars. This already shows the robustness of the modified algorithm to statistical noise. We would like to highlight here that the unitary state evolution (following equation (10)) is done in preparation. The noise is added to the measurement, not the preparation. Infidelities below 10% are achieved within around 15 iterations, four times more than in the baseline measurement with high count rates (see table 1 for details).

We furthermore studied the performance of MEG under high statistical noise, but using generalised Pauli operator measurements rather than MUBs, shown in figure 1(c). As generalised Pauli operators can be mathematically defined, using them instead of MUBs is a powerful tool to describe states far beyond the qubit. We observe that state estimation and online tracking are again in excellent agreement and the overall mean infidelity $\sim 5.1\%$ is slightly better than in the MUB case, but overlapping within uncertainty bars. This demonstrates that generalised Pauli measurements are a viable path to extend MEG towards arbitrary high dimensions in realistic experimental settings. The initial convergence towards the unknown state is slower with around 25 iterations necessary to reach an infidelity of 10%. This is to be expected as MUBs span the qutrit state space more efficiently compared to the Pauli operator measurements. Table 1 shows details of the performance.

Since a changing state leads to changing probabilities of finding a system in a particular state, we also show that we are able to follow these probabilities. Figure 2 illustrates one example of these probabilities $p_i = |\langle i | \psi_t \rangle|^2$ for the logical basis states $|i\rangle$, $i = 0, 1, 2$, out of the 50 randomly chosen qutrits analysed in figure 1 using MUBs. The theoretically expected probabilities in the experiment (dashed lines) are followed nicely by online state tracking of the deterministic evolution in the experiment (solid lines). This confirms that the low infidelities directly correspond to the capability to predict measurement outcomes on the states well. We also highlight that MEG quickly converges to a useful estimate (after 3–4 iterations), even though the initial guess is a completely mixed qutrit ($p_i = 1/3 \forall i$) to avoid bias in the results. The small offset between theory and experiment could be further decreased by using an adaptive learning rate.

3.2. Noisy MEG

We tested the efficacy of MEG under significant environmental noise experimentally—by adding a light bulb close to the detector while keeping the signal rate at $N \approx 10^2$ photons per measurement—and in simulations—adding Poissonian distributed noise to the raw data. The strength of the noise in the experiment is controlled via the distance and angle of the light bulb to the single photon detector. As a proof of principle demonstration, we only looked at stationary states using MUBs in our experiment, yet the simulations show similar behaviour for all estimation and online tracking scenarios investigated in the



previous section. The median infidelities of 50 randomly chosen states for different methods (solid—experiment, dashed—simulation) and environmental noise strengths (colours) are shown in figure 3. Shaded uncertainty ranges similar to figure 1 are omitted for clarity. As expected, the achievable infidelity and number of iterations to get there both become higher as the environmental noise increases, however, MEG is showing exceptional robustness.

We observe that up to $N_{back} \approx 2$ kHz of experimental and simulated noise (not shown explicitly in the figure), the infidelities are comparable to the *no noise* case within uncertainty bars. This corresponds to a $SNR \approx 0.05$, so only one in 20 photons carry the actual information on the unknown quantum state prepared in the experiment. Here and in figure 3, N_{back} relates purely to environmental noise from the light bulb, excluding other noise sources like e.g. dark counts. It is however noteworthy that even at 0 kHz of artificially introduced noise, the naturally occurring counting noise together with background and dark count rates are almost double the signal count rate, i.e. ~ 170 compared to ~ 100 photons per measurement. Experimental and simulated data for $N_{back} = [1, 2.5]$ kHz show good overlap within uncertainty bars, indicating the validity of the noise model in simulation. Therefore we expect to achieve infidelities of around 10% up to $SNR \approx 0.01$ (orange dashed line). The seemingly smoother performance of the simulations stems from 20 runs of randomly added shot-to-shot noise for each of the 50 investigated states. In other words, the results from simulations reflect the median infidelity of $50 \times 20 = 1000$ traces, compared to 50 in the experiment.

4. Discussion

We have presented an efficient tomography algorithm to track the continuous evolution of quantum states despite significant environmental noise. Our approach, MEG tomography, uses machine learning techniques to iteratively update an estimate of a quantum state in real time. We have extended the original online tomography proposal [14] to arbitrary high-dimensional systems (qudits) and experimentally demonstrated the algorithm with a qutrit encoded in the shape of photons. We have shown that MEG is highly resilient to noise: we are able to estimate the quantum state with high fidelities, and accurately predict probabilities of measurement outcomes for different types of evolution and signal strengths.

Although very useful, online QST of dynamical and/or noisy quantum states is a fairly new and mostly unexplored research area. Theoretical proposals cover either noisy environments [20] or evolving states [34–36], but we are not aware of any investigations into the robustness of tracking dynamical states with high noise in any of the proposed algorithms. More recently, there have been some experimental demonstrations of state tracking [10, 37] which naturally involves some noise due to the statistical nature of measurements. However, neither of these works explicitly mentions or characterises the performance under changing or high noise explored in our work. As discussed in [14], MEG can be used to estimate any type of

quantum state. This includes mixed states as well as entangled states, as long as the measurements are from an informationally-complete set. Our robust technique will enable applications that benefit from efficient online tomography, e.g. quantum process tomography [38, 39] and quantum error mitigation [40]/correction [41].

Our results can be extended to process tomography through the Choi-Jamiołkowski isomorphism [42, 43], which allows us to represent a channel using a quantum state that lives in a d^2 -dimensional Hilbert space. In this case, the process estimation becomes state estimation, and MEG could be utilised for the procedure. This provides a more efficient solution compared to standard process tomography which requires computational complexity $O(d^8)$ by using a tomographically complete set of states in preparation and measurement, even $O(d^{10})$ for an over-complete set [44]. The bottleneck of the standard procedure comes from the matrix-vector multiplications required for the estimation procedure. On the other hand, for the MEG update rule, the bottleneck operation is the matrix exponential which is computationally more efficient (see [14] and references within).

On the theoretical side, there are many interesting extensions to this work. One direction is exploring the use of continuous monitoring (weak measurements) combined with MEG. This can have applications in quantum control where we want to track an evolving state without completely collapsing it. Another extension is to study the theoretical convergence of MEG [14] to state tracking (time-varying true states), as well as the case of including the additional projection step for pure state estimation. Intuitively, the good performance of MEG can be thought of to be similar to that of a moving-average filter, where noise gets averaged out over time. The effect is comparable to increasing the number of shots per measurement over many measurements. A more rigorous analysis could be done as future work. Finally, a convergence analysis of simple models such as the example given in equation (7) can also provide more insight on the theoretical performance of MEG.

Data availability statement

The source code for the proposed theoretical methods is publicly available on github at https://github.com/akramyousry/MEG_state_tracking.

The data that support the findings of this study are openly available at the following URL/DOI: https://figshare.com/projects/Efficient_Tracking_of_Noisy_Quantum_States/130433.

Acknowledgments

The authors thank Daniel Oi for constructive discussions. This research was supported by the Australian Research Council Centre of Excellence for Engineered Quantum Systems (EQUS, CE170100009) and Discovery Project (DP200102273). A Y is supported by an Australian Government Research Training Program Scholarship, and the Australian Research Council under the Centre of Excellence Scheme No. CE170100012. M T is supported by the National Research Foundation, Prime Minister's Office, Singapore and the Ministry of Education, Singapore under the Research Centres of Excellence programme, and by NUS startup Grant Nos. (R-263-000-E32-133 and R-263-000-E32-731). J R is supported by a Westpac Bicentennial Foundation Research Fellowship.

ORCID iDs

Markus Rambach  <https://orcid.org/0000-0002-4659-3804>

Akram Youssry  <https://orcid.org/0000-0001-7301-5834>

References

- [1] Paris M and Řeháček J (eds) 2004 *Quantum State Estimation (Series Lecture Notes in Physics vol 649)* (Berlin: Springer)
- [2] Haah J, Harrow A W, Ji Z, Wu X and Yu N 2017 Sample-optimal tomography of quantum states *IEEE Trans. Inf. Theory* **63** 5628–41
- [3] D'Ariano G M, Paris M G and Sacchi M F 2003 Quantum tomography *Advances in Imaging and Electron Physics* vol 128 ed P W Hawkes (Amsterdam: Elsevier) pp 205–308
- [4] Opatrný T, Welsch D-G and Vogel W 1997 Least-squares inversion for density-matrix reconstruction *Phys. Rev. A* **56** 1788
- [5] Aaronson S, Chen X, Hazan E, Kale S and Nayak A 2019 Online learning of quantum states *J. Stat. Mech.* **124019**
- [6] Granade C, Combes J and Cory D G 2016 Practical Bayesian tomography *New J. Phys.* **18** 033024
- [7] Lin C-M, Hsu Y-M and Li Y-H 2020 An online algorithm for maximum-likelihood quantum state tomography (arXiv:2012.15498)
- [8] Qi B, Hou Z, Wang Y, Dong D, Zhong H-S, Li L, Xiang G-Y, Wiseman H M, Li C-F and Guo G-C 2017 Adaptive quantum state tomography via linear regression estimation: theory and two-qubit experiment *npj Quantum Inf.* **3** 19
- [9] Chen Y and Wang X 2020 More practical and adaptive algorithms for online quantum state learning (arXiv:2006.01013)
- [10] Nohara S, Okamoto R, Fujiwara A and Takeuchi S 2020 Adaptive quantum state estimation for dynamic quantum states *Phys. Rev. A* **102** 030401

- [11] Quek Y, Fort S and Ng H K 2021 Adaptive quantum state tomography with neural networks *npj Quantum Inf.* **7** 105
- [12] Ferrie C 2014 Self-guided quantum tomography *Phys. Rev. Lett.* **113** 190404
- [13] Li Y-H and Cevher V 2019 Convergence of the exponentiated gradient method with armijo line search *J. Optim. Theory Appl.* **181** 588
- [14] Youssry A, Ferrie C and Tomamichel M 2019 Efficient online quantum state estimation using a matrix-exponentiated gradient method *New J. Phys.* **21** 033006
- [15] Zhang K, Cong S, Li K and Wang T 2020 An online optimization algorithm for the real-time quantum state tomography *Quantum Inf. Process.* **19** 361
- [16] Silberfarb A, Jessen P S and Deutsch I H 2005 Quantum state reconstruction via continuous measurement *Phys. Rev. Lett.* **95** 030402
- [17] Shabani A, Roden J and Whaley K B 2014 Continuous measurement of a non-markovian open quantum system *Phys. Rev. Lett.* **112** 113601
- [18] Cole J H, Schirmer S G, Greentree A D, Wellard C J, Oi D K L and Hollenberg L C L 2005 Identifying an experimental two-state Hamiltonian to arbitrary accuracy *Phys. Rev. A* **71** 062312
- [19] Anshu A, Arunachalam S, Kuwahara T and Soleimanifar M 2021 Sample-efficient learning of interacting quantum systems *Nat. Phys.* **17** 931
- [20] Bogdanov Y I, Bantysh B I, Bogdanova N A, Kvasnyy A B and Lukichev V F 2016 Quantum states tomography with noisy measurement channels *Proc. SPIE* **10224** 102242O
- [21] Ivanova-Rohling V N, Rohling N and Burkard G 2022 Optimal quantum state tomography with noisy gates (arXiv:2203.05677)
- [22] Farooq A, Khalid U, ur Rehman J and Shin H 2022 Robust quantum state tomography method for quantum sensing *Sensors* **22** 2669
- [23] Blume-Kohout R 2010 Optimal, reliable estimation of quantum states *New J. Phys.* **12** 043034
- [24] Allen L, Barnett S M and Padgett M J 2016 *Optical Angular Momentum* (Boca Raton, FL: CRC Press)
- [25] Langford N K, Dalton R B, Harvey M D, O'Brien J L, Pryde G J, Gilchrist A, Bartlett S D and White A G 2004 Measuring entangled qutrits and their use for quantum bit commitment *Phys. Rev. Lett.* **93** 053601
- [26] Rambach M, Qaryan M, Kewning M, Ferrie C, White A G and Romero J 2021 Robust and efficient high-dimensional quantum state tomography *Phys. Rev. Lett.* **126** 100402
- [27] Durt T, Englert B-G, Bengtsson I and Życzkowski K 2010 On mutually unbiased bases *Int. J. Quantum Inf.* **08** 535
- [28] Wootters W K and Fields B D 1989 Optimal state-determination by mutually unbiased measurements *Ann. Phys.* **191** 363–81
- [29] Kimura G 2003 The bloch vector for N-level systems *Phys. Lett. A* **314** 339
- [30] Aaronson S 2018 Shadow tomography of quantum states *Proc. 50th Annual ACM SIGACT Symp. on Theory of Computing* pp 325–38
- [31] Struchalin G, Zagorovskii Y A, Kovlakov E, Straupe S and Kulik S 2021 Experimental estimation of quantum state properties from classical shadows *PRX Quantum* **2** 010307
- [32] Thew R T, Nemoto K, White A G and Munro W J 2002 Qudit quantum-state tomography *Phys. Rev. A* **66** 012303
- [33] Bogdanov Y I 2009 Unified statistical method for reconstructing quantum states by purification *J. Exp. Theor. Phys.* **108** 928
- [34] Cramer M, Plenio M B, Flammia S T, Somma R, Gross D, Bartlett S D, Landon-Cardinal O, Poulin D and Liu Y-K 2010 Efficient quantum state tomography *Nat. Commun.* **1** 149
- [35] Czerwinski A 2020 Dynamic state reconstruction of quantum systems subject to pure decoherence *Int. J. Theor. Phys.* **59** 3646
- [36] Chen X, Hazan E, Li T, Lu Z, Wang X and Yang R 2022 Adaptive online learning of quantum states (arXiv:2206.00220)
- [37] Lanyon B P et al 2017 Efficient tomography of a quantum many-body system *Nat. Phys.* **13** 1158
- [38] Chuang I L and Nielsen M A 1997 Prescription for experimental determination of the dynamics of a quantum black box *J. Mod. Opt.* **44** 2455
- [39] O'Brien J L, Pryde G J, Gilchrist A, James D F V, Langford N K, Ralph T C and White A G 2004 Quantum Process tomography of a controlled-NOT gate *Phys. Rev. Lett.* **93** 080502
- [40] Endo S, Benjamin S C and Li Y 2018 Practical quantum error mitigation for near-future applications *Phys. Rev. X* **8** 031027
- [41] Lidar D A and Brun T A (ed) 2012 *Quantum Error Correction* (Cambridge: Cambridge University Press)
- [42] Jamiolkowski A 1972 Linear transformations which preserve trace and positive semidefiniteness of operators *Rep. Math. Phys.* **3** 275
- [43] Choi M-D 1975 Completely positive linear maps on complex matrices *Linear Algebr. Appl.* **10** 285–90
- [44] Knee G C, Bolduc E, Leach J and Gauger E M 2018 Quantum process tomography via completely positive and trace-preserving projection *Phys. Rev. A* **98** 062336